IOP Conf. Series: Journal of Physics: Conf. Series **871** (2017) 012001 doi:10.1088/1742-6596/871/1/012001

Paramagnetic and diamagnetic pair-breaking effect in electric-field-induced surface superconductivity under parallel magnetic fields

Masanori Ichioka[1,2], Masahiro Nabeta[1], Kenta K Tanaka[1] and Seiichiro Onari[1,2]

[1] Department of Physics, Okayama University, Okayama 700-8530, Japan
[2] Research Institute for Interdisciplinary Science (RIIS), Okayama University, Okayama 700-8530, Japan

E-mail: ichioka@okayama-u.ac.jp

Abstract. Electric-field-induced surface superconductivity is studied by Bogoliubov-de Gennes equation under magnetic fields parallel to the surface. We estimate the pair-breaking effects by the paramagnetic Zeeman shift and by diamagnetic screening current. We find that the depth dependences of pair potential, screening current, spin current, and paramagnetic moment under the magnetic fields reflect the multi-gap superconductivity in the sub-band structure.

1. Introduction

By strong electric field of the field-effect-transistor or the electric-double-layer-transistor, carriers are induced and trapped in the confinement potential of the electric field near the surface of insulators or semiconductors. In the surface metallic states, superconductivity appears at low temperature [1], as performed in $SrTiO_3$ [2], ZrNCl [3], $KTaO_3$ [4], and MoS_2 [5, 6]. A unique nature of the surface metallic state is that sub-bands are formed by the quantum confinement of carriers near the surface due to the strong electric field [2, 7, 8]. By a previous theoretical study, the surface superconductivity is expected to be multi-gap superconductivity depending on the sub-bands [9]. The multi-gap structure of sub-band system is related to the depth-dependence of the superconducting state.

In order to examine properties reflecting the multi-gap superconductivity in the electric-field-induced surface metallic state, we theoretically study electronic states when magnetic fields are applied parallel to the surface. In this configuration, experimental observation of the upper critical field H_{c2} suggests that vortices do not penetrate into the superconducting region near the surface [10]. The effects of parallel magnetic fields on the superconductivity occur by two contributions of paramagnetic and diamagnetic pair-breakings. Under the magnetic field, Fermi surface is split between up- and down-spin electrons. This split induces paramagnetic moment and the paramagnetic pair-breaking of the superconductivity. In reference [11], the paramagnetic pair-breaking effect was reported in the surface superconductivity in the confinement potential including screening effect of electric fields by carriers. On the other hand, by the contribution of vector potential, screening supercurrent flows near the surface so that magnetic field is

decreased inside the superconducting region. The diamagnetic pair-breaking occurs by the flow of supercurrent.

In this work, wave functions in the superconducting states are calculated from Bogoliubov-de Gennes (BdG) equation, assuming s-wave pairing interaction [9, 12]. Here, we concentrate on the case when confinement potential by electric field is given by triangular potential. We study spatial structure of the superconducting state under parallel magnetic fields, and estimate effects of paramagnetic and diamagnetic pair-breakings comparatively in the pair potential, screening current, spin current and paramagnetic moment. By the sub-band decomposition of these quantities, we can see properties of multi-gap superconductivity, because superconductivity in higher-level sub-band is more suppressed with increasing magnetic fields.

This paper is organized as follows. After the introduction, we explain our theoretical formulation by the BdG equation under parallel magnetic fields in section 2. We study the depth z dependence of pair potential $\Delta(z)$, supercurrent $J(z)$, and spin current $J_s(z)$ in section 3. The z-dependence of paramagnetic moment $m(z)$ is studied in section 4. Last section is devoted to summary.

2. Formulation by BdG equation

We use coordinate $\mathbf{r} = (x, y, z)$, where z (≥ 0) is depth from the surface at $z = 0$. The confinement potential near the surface is assumed to be triangular potential $V(z) = |e|F_0 z$. We typically consider the case of sheet carrier density $n_{2\mathrm{D}} = 6.5 \times 10^{13}[\mathrm{cm}^{-2}]$, electric field $F_0 = 1.4 \times 10^{-3}[\mathrm{V/nm}]$, and single band with effective mass $m^* = 4.8m_0$, where m_0 is free electron's mass. This corresponds to one of the cases in reference [9].

Solving the BdG equation [12], we determine the pair potential $\Delta(\mathbf{r})$, and the wave functions $u_\epsilon(\mathbf{r})$, $v_\epsilon(\mathbf{r})$ for the eigen-energy E_ϵ. When we consider diamagnetic current, we set the vector potential as $\mathbf{A} = (0, A_y, 0)$ with $A_y = -Hz$, so that the magnetic field parallel to the surface is applied along the x direction, and the screening current flows along the y direction. In this situation, we can set $\Delta(\mathbf{r}) = \Delta(z)\mathrm{e}^{\mathrm{i}2qy}$ and

$$\begin{pmatrix} u_\epsilon(\mathbf{r}) \\ v_\epsilon(\mathbf{r}) \end{pmatrix} = \frac{1}{\sqrt{S}}\mathrm{e}^{\mathrm{i}(k_x x + k_y y)} \begin{pmatrix} u_\epsilon(z)\mathrm{e}^{\mathrm{i}qy} \\ v_\epsilon(z)\mathrm{e}^{-\mathrm{i}qy} \end{pmatrix}, \tag{1}$$

where S is unit area of surface. Thus the BdG equation is reduced to

$$\begin{pmatrix} K_+ & \Delta(z) \\ \Delta(z) & -K_- \end{pmatrix} \begin{pmatrix} u_\epsilon(z) \\ v_\epsilon(z) \end{pmatrix} = E_\epsilon \begin{pmatrix} u_\epsilon(z) \\ v_\epsilon(z) \end{pmatrix}, \tag{2}$$

with the kinetic term

$$K_\pm = \frac{\hbar^2}{2m^*}\left(k_x^2 + (\pm k_y + q + \frac{\pi}{\phi_0}A_y)^2 - \partial_z^2\right) + V(z) \mp \mu_\mathrm{B}H - \mu, \tag{3}$$

where ϕ_0 is a flux quanta, and $\pm\mu_\mathrm{B}H$ is Zeeman energy with the Bohr magneton $\mu_\mathrm{B} = 5.7883 \times 10^{-5}$ [eV/T]. The eigen-states of equation (2) are labeled by $\epsilon \equiv (k_x, k_y, i_z)$. i_z ($= 1,\ 2,\ \cdots$) indicates label for sub-bands coming from quantization by confinement in the z-direction. As the boundary condition at the surface $z = 0$, we set $u_\epsilon(z) = v_\epsilon(z) = 0$. Throughout this paper, energy, length, magnetic field, and local carrier densities are, respectively, presented in unit of eV, nm, T, and nm^{-3}. The chemical potential μ is determined to fix the carrier density as

$$n_{2\mathrm{D}} = \int_0^\infty \{n_\uparrow(z) + n_\downarrow(z)\}\,\mathrm{d}z, \tag{4}$$

where local carrier density for up- and down-spins are, respectively, given by

$$n_\uparrow(z) = \sum_\epsilon |u_\epsilon(z)|^2 f(E_\epsilon), \quad n_\downarrow(z) = \sum_\epsilon |v_\epsilon(z)|^2 f(-E_\epsilon) \tag{5}$$

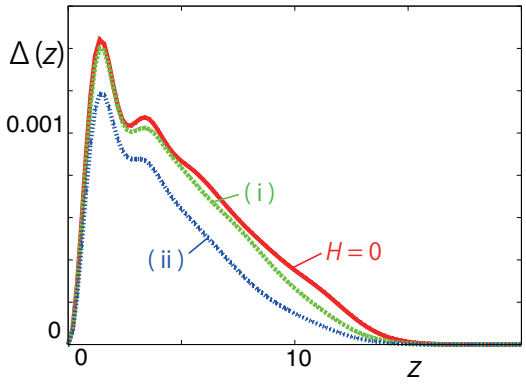

Figure 1. Profile of pair potential $\Delta(z)$ as a function of depth z. Solid line is for a zero magnetic field. Dashed lines are for $H = 10$ in the cases (i) and (ii) explained in text.

from the eigen states, with the Fermi distribution function $f(E)$.

The pair potential is calculated by the gap equation

$$\Delta(z) = V_{\rm pair} \sum_{\epsilon}{}' u_\epsilon(z) v_\epsilon(z) f(-E_\epsilon). \tag{6}$$

In equation (6), the energy cutoff $E_{\rm cut}$ of the pairing interaction is considered in the summation $\sum'$. Here, we consider a conventional case of spin-independent isotropic s-wave pairing. We typically use $V_{\rm pair} = 0.08$, and $E_{\rm cut} = 0.01$. Iterating calculations of equations (2) and (6), we obtain selfconsistent results of $\Delta(z)$ and wave functions. We study the superconducting state at low temperature $T = 1.16 \times 10^{-2}$K $\ll T_{\rm c}$ and $H = 10$T.

To study effects of paramagnetic and diamagnetic pair-breakings under parallel magnetic fields, we perform calculations in the following two cases.

Case (i): We neglect the diamagnetic effect, setting $A_y = q = 0$, and consider only the paramagnetic effect. This is to clarify contributions of the paramagnetic pair-breaking effect.

Case (ii): We consider both diamagnetic and paramagnetic pair-breaking effects, setting $A_y = -Hz$. q is tuned to satisfy the current conservation $\int_0^\infty J(z){\rm d}z = 0$ with local screening current density along the y direction, $J(z) = J_\uparrow(z) + J_\downarrow(z)$. The up- and down-spin contributions are, respectively, calculated as

$$J_\uparrow(z) = \frac{e\hbar}{2m} \sum_\epsilon \left(k_y + q + \frac{\pi}{\phi_0} A_y \right) |u_\epsilon(z)|^2 f(E_\epsilon), \tag{7}$$

$$J_\downarrow(z) = \frac{e\hbar}{2m} \sum_\epsilon \left(-k_y + q + \frac{\pi}{\phi_0} A_y \right) |v_\epsilon(z)|^2 f(-E_\epsilon) \tag{8}$$

from the eigen states. From comparison of the cases (i) and (ii), we find contributions of diamagnetic pair-breaking effect in the surface superconductivity.

3. Depth dependence of pair potential, screening current, and spin current

To study the pair-breaking effects by parallel magnetic fields, we compare the spatial structure of superconductivity at a magnetic field $H = 10$ and a zero field. The critical field to the normal state is the first order transition at $H \sim 12$. In figure 1, we present the profile of pair potential $\Delta(z)$ obtained from selfconsistent calculation of BdG equation in the cases (i) and (ii). Compared to the zero field case, we see suppression of $\Delta(z)$ under magnetic field $H = 10$. In the

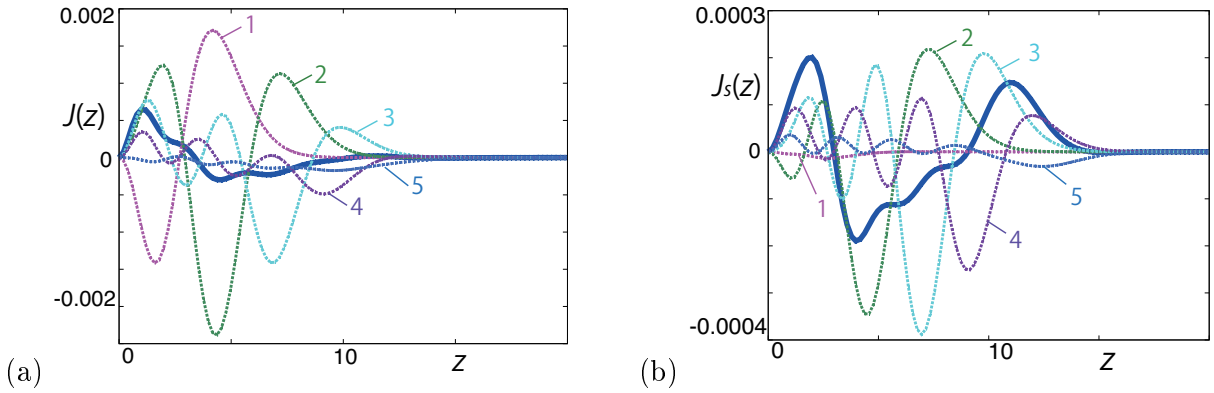

Figure 2. (a) Local current density $J(z) = J_\uparrow(z) + J_\downarrow(z)$ and (b) local spin current density $J_s(z) = J_\uparrow(z) - J_\downarrow(z)$ are presented by solid lines as a function of depth z at $H = 10$ in the case (ii). Dashed lines indicate contributions from i_z-th sub-band to $J(z)$ and $J_s(z)$. i_z =1, 2, $\cdots$, 5.

case (i) considering only paramagnetic pair-breaking effect, the suppression of $\Delta(z)$ is eminent at deeper z region. In the case (ii) considering both paramagnetic and diamagnetic pair-breaking effects, $\Delta(z)$ is further suppressed than that in case (i) due to the additional pair-breaking effect by the diamagnetic current. In this case, we see the suppression until smaller z region.

Profile of the diamagnetic screening current $J(z)$ along the y-direction parallel to the surface is presented by a solid line in figure 2(a) for the case (ii). Near the surface $z \sim 0$, $J(z) > 0$ to suppress the penetration of the magnetic field from the surface side. On the other hand, $J(z) < 0$ at $z \sim 5$ to screen the magnetic field from the deeper side of the superconducting region. The sub-band contributions to $J(z)$ are calculated by restricting the ϵ-summation to one sub-band i_z. In figure 2(a), sub-band contributions from lower three sub-bands $i_z = 1$, 2, 3 are large. By the summation of the oscillating wave function of the sub-band contributions, profile of $J(z)$ is constructed. We see small positive $J(z)$ at $z \sim 11$.

When both paramagnetic and diamagnetic pair-breaking effects work, there appears spin current $J_s(z) = J_\uparrow(z) - J_\downarrow(z)$, as shown in figure 2(b) for the case (ii). In the sub-band decomposition of $J_s(z)$, contributions from $i_z = 2$, 3, 4 are dominant. We note that contribution from lowest sub-band $i_z = 1$ is very small, because superconductivity at the sub-band $i_z = 1$ is not broken as seen later in figure 3(b).

4. Depth dependence of paramagnetic moment

In the presence of Zeeman shift, local paramagnetic moment $m(z) = n_\uparrow(z) - n_\downarrow(z)$ appears, as shown in figure 3. The moment $m(z)$ comes from contribution of sub-bands where superconductivity is largely suppressed, and electronic state becomes normal-state-like with small superconductivity. When diamagnetic pair-breaking effect is neglected, $m(z)$ consists of contributions from higher-level sub-bands $i_z = 4$ and 5, as shown in figure 3(a) for the case (i). Thus $m(z)$ has a main peak at a deep position $z \sim 11$. There are no contributions from lower-level sub-bands $i_z = 1$, 2, 3, where superconductivity is not yet broken. If the diamagnetic pair-breaking effect is included as in figure 3(b) for the case (ii), contributions from sub-bands $i_z = 2$ and 3 also appear in $m(z)$. Therefore region of large $m(z)$ extends towards smaller z, and $m(z)$ becomes larger compared to the case of figure 3(a). Even in this case, lowest sub-band $i_z = 1$ gives no contributions to $m(z)$ since it keeps large superconductivity.

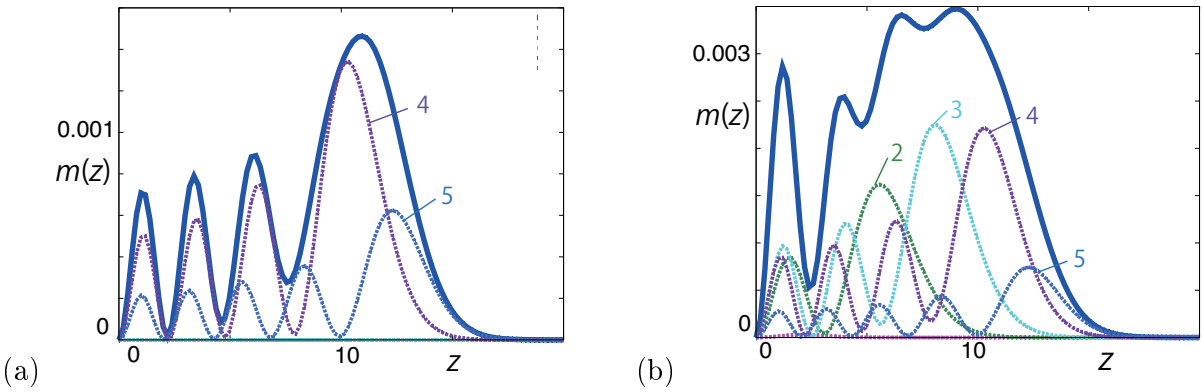

Figure 3. Local paramagnetic moment $m(z) = n_\uparrow(z) - n_\downarrow(z)$ is presented by solid lines as a function of depth z at $H = 10$. (a) The case (i) considering only paramagnetic pair-breaking effect. (b) The case (ii) including both paramagnetic and diamagnetic pair-breaking effects. Dashed lines indicate contributions from i_z-th sub-band to $m(z)$.

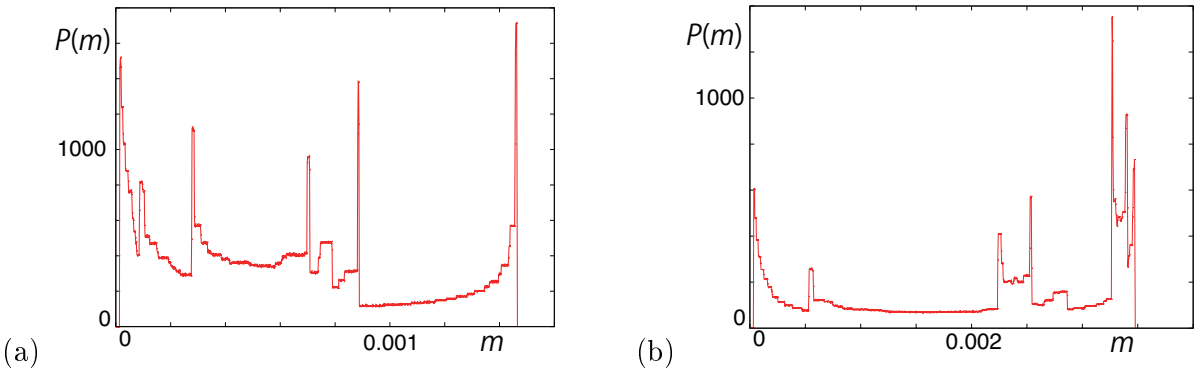

Figure 4. Distribution $P(m)$ estimated from $m(z)$ at $H = 10$. (a) The case (i) with paramagnetic effect only, obtained from figure 3(a). (b) The case (ii) with both paramagnetic and diamagnetic effects, obtained from figure 3(b).

We also calculate distribution of $m(z)$ as

$$P(m) = \int_0^\infty \delta(m - m(z))\mathrm{d}z, \tag{9}$$

which gives volume satisfying $m = m(z)$. $P(m)$ in figures 4(a) and 4(b) are, respectively, calculated from figures 3(a) and 3(b). Peaks in $P(m)$ come from local maximum or local minimum of $m(z)$ in figure 3. In the case (ii), because $m(z)$ has large value at many local minimum positions, weight of $P(m)$ is located at higher m in figure 4(b), compared to that in figure 4(a). The distribution $P(m)$ corresponds to the NMR or μSR spectra in bulk superconductors. In the surface superconductivity, NMR spectrum may selectively detect local $m(z)$ depending position z of nuclei used in NMR experiments.

5. Summary

Solving BdG equation selfconsistently, we studied paramagnetic and diamagnetic pair-breaking effects in electric-field-induced surface superconductivity under parallel magnetic fields. With

increasing magnetic fields, superconductivity in higher-level sub-bands is suppressed and becomes normal-state-like with small superconductivity. We found that sub-band contributions to the pair potential and screening current dominantly come from lower-level sub-bands keeping large superconductivity. On the other hand, main contributions to paramagnetic moment and spin current are from occupied higher-level sub-bands with partially suppressed superconductivity. These properties come from multi-gap structure of superconductivity in the sub-band system of the surface metallic states.

Acknowledgments

This work was supported by JSPS KAKENHI Grant Number 25400373.

References

[1] Ueno K, Shimotani H, Yuan H, Ye J T, Kawasaki M and Iwasa Y 2014 *J. Phys. Soc. Jpn.* **83** 032001
[2] Ueno K, Nakamura S, Shimotani H, Ohtomo A, Kimura N, Nojima T, Aoki H, Iwasa Y and Kawasaki M 2008 *Nature Mater.* **7** 855
[3] Ye J T, Inoue S, Kobayashi K, Kasahara Y, Yuan H T, Shimotani H and Iwasa Y 2011 *Nature Mater.* **9** 125
[4] Ueno K, Nakamura S, Shimotani H, Yuan H T, Kimura N, Nojima T, Aoki H, Iwasa Y and Kawasaki M 2011 *Nature Nanotechnol.* **6** 408
[5] Taniguchi K, Matsumoto A, Shimotani H and Takagi H 2012 *Appl. Phys. Lett.* **101** 042603
[6] Ye J T, Zhang Y J, Akashi R, Bahramy M S, Arita R and Iwasa Y 2012 *Science* **338** 1193
[7] Santander-Syro A F, Copie O, Kondo T, Fortuna F, Pailhès S, Weht R, Qiu X G, Bertran F, Nicolaou A, Taleb-Ibrahimi A, Le Fèvre P, Herranz G, Bibes M, Reyren N, Apertet Y, Lecoeur P, Barthélémy A and Rozenberg M J 2011 *Nature* **469** 189
[8] King P D C, Walker S M, Tamai A, De la Torre A, Eknapakul T, Buaphet P, Mo S-K, Meevasana W, Bahramy M S and Baumberger F 2014 *Nat. Commun.* **5** 3414
[9] Mizohata Y, Ichioka M and Machida K 2013 *Phys. Rev.* B **87** 014505
[10] Ueno K, Nojima T, Yonezawa S, Kawasaki M, Iwasa Y and Maeno Y 2014 *Phys. Rev.* B **89** 020508
[11] Nabeta M, Tanaka K K, Onari S and Ichioka M 2016 *Physica* C **530** 8
[12] De Gennes P G 1989 *Superconductivity of Metals and Alloys* (Reading, Massachusetts: Addison-Wesley)